JOURNAL OF BACTERIOLOGY, Jan. 2007, p. 633–645 Vol. 189, No. 2
0021-9193/07/$08.00+0 doi:10.1128/JB.00991-06

Mutants, Suppressors, and Wrinkled Colonies: Mutant Alleles of the Cell Division Gene *ftsQ* Point to Functional Domains in FtsQ and a Role for Domain 1C of FtsA in Divisome Assembly▽†

Nathan W. Goehring, Ivana Petrovska, Dana Boyd, and Jon Beckwith*

Department of Microbiology and Molecular Genetics, Harvard Medical School, 200 Longwood Avenue, Boston, Massachusetts 02115

Received 6 July 2006/Accepted 8 September 2006

Cell division in *Escherichia coli* requires the concerted action of at least 10 essential proteins. One of these proteins, FtsQ, is physically associated with multiple essential division proteins, including FtsK, FtsL, FtsB, FtsW, and FtsI. In this work we performed a genetic analysis of the *ftsQ* gene. Our studies identified C-terminal residues essential for FtsQ's interaction with two downstream proteins, FtsL and FtsB. Here we also describe a novel screen for cell division mutants based on a wrinkled-colony morphology, which yielded several new point mutations in *ftsQ*. Two of these mutations affect localization of FtsQ to midcell and together define a targeting role for FtsQ's α domain. Further characterization of one localization-defective mutant protein [FtsQ(V92D)] revealed an unexpected role in localization for the first 49 amino acids of FtsQ. Finally, we found a suppressor of FtsQ(V92D) that was due to a point mutation in domain 1C of FtsA, a domain previously implicated in the recruitment of divisome proteins. However, despite reports of a potential interaction between FtsA and FtsQ, suppression by FtsA(I143L) is not mediated via direct contact with FtsQ. Rather, this mutation acts as a general suppressor of division defects, which include deletions of the normally essential genes *zipA* and *ftsK* and mutations in FtsQ that affect both localization and recruitment. Together, these results reveal increasingly complex connections within the bacterial divisome.

Cell division in a gram-negative bacterium requires the coordinated remodeling of the three-layer cell envelope. Mechanisms must exist to synthesize septal peptidoglycan, provide constrictive force, and effect the membrane fusion and scission events that are required to separate the nascent daughter cells. In *Escherichia coli*, at least 15 proteins have been implicated in this process, and all of these proteins localize to a ring-like structure at midcell commonly referred to as the divisome (5, 20, 39). FtsZ, a tubulin homologue, polymerizes into a ring or tight spiral at the division site (the Z-ring) (2, 35). This structure requires two essential FtsZ-binding proteins, FtsA and ZipA, which cooperate to stabilize the Z-ring and tether it to the inner membrane (29, 30). Once established, the Z-ring can be used as a scaffold for the assembly of the remaining late division proteins.

The remaining "late" division proteins localize to the Z-ring according to a linear hierarchy (→FtsK→FtsQ→FtsL/B→FtsW→FtsI→FtsN), in which a given protein requires the proteins that localize upstream and is, in turn, required for the localization of proteins further downstream. This hierarchy, however, does not represent a true assembly pathway in which the proteins are added to the divisome in sequence. In fact, most of these proteins can associate independent of their normal recruitment to the Z-ring (6, 21).

FtsQ is recruited at an intermediate point in this hierarchy. It requires both the Z-ring components (FtsZ, FtsA, and ZipA) and FtsK in order to localize to midcell. FtsQ is, in turn, required for the recruitment of FtsL/B, FtsW, FtsI, and FtsN (8, 9). FtsQ forms a stable complex with at least two of these proteins, FtsL and FtsB (6). This FtsQ-FtsL-FtsB complex in turn can physically associate with FtsW and FtsI to form a large complex of late division proteins (21). Finally, the finding that FtsQ, when it is prematurely targeted to the Z-ring, can backrecruit FtsK under conditions in which FtsK does not normally localize suggests that there may be a direct interaction between these proteins as well (21). This association is presumably the dominant mechanism for targeting the FtsQ-FtsL-FtsB complex to midcell.

Little is known about the ultimate function of FtsQ in the division process. This protein has been implicated in peptidoglycan synthesis, both because of its absence in bacteria that do not contain a cell wall and because of its very weak homology to Mpl (murein peptide ligase) (4). There is, however, no experimental evidence to support these suggestions. Although FtsQ has been the subject of several genetic studies, the resulting mutants have provided little information about its specific function (10, 24). Analysis of these mutants in combination with several genetic and biochemical assays has nonetheless begun to shed light on the domains of FtsQ that are responsible for its interactions with other members of the divisome.

FtsQ is a bitopic membrane protein with a short cytoplasmic domain, a single transmembrane segment, and a large periplasmic domain (Fig. 1A). The cytoplasmic and transmembrane domains (amino acids 1 to 49) are not essential and can be readily replaced by the corresponding 5′ region of the unre-

* Corresponding author. Mailing address: Department of Microbiology and Molecular Genetics, Harvard Medical School, 200 Longwood Avenue, Boston, MA 02115. Phone: (617) 432-1920. Fax: (617) 738-7664. E-mail: jon_beckwith@hms.harvard.edu.

† Supplemental material for this article may be found at http://jb.asm.org/.

▽ Published ahead of print on 15 September 2006.

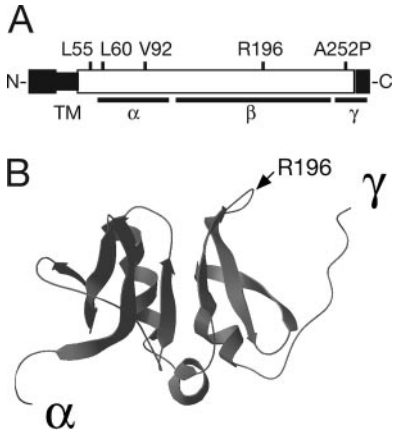

FIG. 1. Structure and topology of FtsQ. (A) The positions of the transmembrane (TM) segment and α, β, and γ domains described by Robson and King (32) are indicated. Nonessential regions are indicated by solid boxes and include the membrane anchor and the extreme C terminus. The relative positions of the mutations described in this paper are indicated. (B) Structure of the *cis* conformer of the β domain of the FtsQ homologue DivIB. Connections to the α and γ domains are indicated, as is the predicted position of R196.

lated protein MalF (24). Truncation of the final 29 amino acids, on the other hand, renders FtsQ nonfunctional. While unable to recruit FtsL and FtsB, this partially defective protein nonetheless localizes normally, indicating that amino acids 50 to 247 are sufficient for targeting to midcell (10).

A structural analysis of DivIB, the *Bacillus subtilis* FtsQ homologue, revealed the existence of three distinct domains, the α, β, and γ domains. The γ domain is sensitive to proteases and unstructured in the absence of other proteins and corresponds roughly to the final 30 amino acids of FtsQ that are required for interaction with FtsL and FtsB (32). This observation raises the possibility that this region becomes structured only when it is incorporated into the FtsQ-FtsL-FtsB complex. The α domain is a discretely folded domain identified bioinformatically as a POTRA repeat-containing domain shared with the Omp85 family of proteins involved in assembly of proteins in the outer membrane (33). Relatives of Omp85 are important components of two-partner secretion systems and the Toc75 family of protein translocases found in plastid outer envelopes. In these cases, POTRA domains interact with peptide substrates prior to translocation across the outer membrane (17). Although the significance of this observation is unclear given that FtsQ is not associated with the outer membrane, it raises the possibility that this domain may play a chaperone-like role. Finally, while the nuclear magnetic resonance structure of the β domain has been determined, the structure does not resemble that of any other known proteins and does not in itself suggest a function (32) (Fig. 1B).

In this work we extend the genetic analysis of FtsQ. Using a directed approach, we identified the minimal complementing length of FtsQ and isolated a point mutation that disrupts the ability of the C-terminal γ domain to interact with FtsL and FtsB. These results indicated that a specific region of the γ domain is essential for recruitment. Here we also describe a novel wrinkled-colony screen for nonlethal division defects, which we used to isolate additional lesions in *ftsQ*. Two of these lesions specifically affect the ability of FtsQ to localize and define a role for the α domain in midcell targeting. Further analysis of one of these mutations, V92D, resulted in discovery of a role for the first 49 amino acids of FtsQ in localization. This region of the protein, consisting of the cytoplasmic and transmembrane domains, was previously shown to be nonessential. Our results suggest that this N-terminal region and the α domain act cooperatively to bring FtsQ to midcell. Finally, characterization of suppressors of the V92D lesion led to isolation of a novel allele of *ftsA*, *ftsA*(*I143*). This mutation is capable of rescuing a broad array of divisome assembly defects, including deletion mutations of *ftsK* or *zipA*, as well as localization and recruitment mutations in FtsQ. Taken together, the results of this genetic analysis along with other recent studies paint an increasingly complex picture of the divisome assembly process.

MATERIALS AND METHODS

Bacterial strains, plasmids, media, and general methods. Bacterial strains and plasmids used in this work are listed in Table 1. All experiments were performed with NZY medium (22). Antibiotics were added when appropriate at the concentrations indicated below. D-Glucose and L-arabinose were each added at a concentration of 0.2% to repress or induce the expression of genes under control of the P_{BAD} promoter. Isopropyl-β-D-thiogalactoside (IPTG) was added at the concentrations indicated below.

Standard laboratory techniques were used for cloning and analysis of DNA, PCR, electroporation, transformation, and P1 transduction (28). Chromosomal constructs were integrated using λInCh (3). Individual bacterial strains and plasmids were constructed as described below or as indicated in Table 1. λ*att* integrated constructs were transduced by P1 using resistance to ampicillin (25 μg/ml). The method used for PCR mutagenesis has been described previously (10). Primer sequences are available upon request.

Cloning and strain construction. FtsQ truncations were amplified from pLMG161, and the resulting PCR products were ligated into the EocRI/XbaI sites of pBAD18. The resulting plasmids were then digested with XbaI/HindIII, and oligonucleotides encoding the c-Myc tag were inserted.

To insert restriction sites (BsiWI, Bsu36I) flanking amino acids 250 to 256, overlapping oligonucleotides encoding the altered sequence were annealed and used to PCR amplify the altered region. Subsequent PCR with outside primers resulted in a full-length *ftsQ* PCR product containing the desired sites. This product was inserted into pNG1 to obtain pNG4. PhoA was amplified from pGA4ΔBsp using primers PhoA5′ and PhoA3′. The fragment was then inserted into XbaI/HindIII sites of pNG4 to create pNG6. Finally, to create pNG17, oligonucleotides encoding an SnaBI site were inserted into the BsiWI/Bsu36I sites of pNG6. Oligonucleotides in which codons 251 to 256 were individually scrambled were ligated into the BsiWI/Bsu36I sites and transformed into *E. coli* DH5α. The resulting transformants were pooled, and mutagenized plasmid pools were miniprepped and digested with SnaBI to eliminate any contaminating parent plasmid before transformation into screening strains.

Plasmid pDSW206-*ftsQ* uses the native *ftsQ* Shine-Delgarno sequence, resulting in very low expression levels. QQQ and FFQ were PCR amplified and ligated into pDSW206-*ftsQ* and pDSW206-*ftsQ*(*V92D*) using the Shine-Delgarno sequence and Met from plasmid pDSW206 to obtain a more comparable expression level between FtsQ and the FFQ swap. QQQ is a previously described swap allele of FtsQ that was used in construction of FFQ and behaves exactly like wild-type FtsQ. The resulting plasmids, pNG198, pNG200, pNG201, and pNG203, were then integrated into the λ*att* site using λInCh.

Linear PCR transformation was performed in the presence of plasmid pKD46 using the protocol of Datsenko and Wanner (13). A linear PCR product encompassing the *ftsQE14*::*kan* allele was introduced into WM1659, which contained the *ftsA*(*R286W*) mutation and a P1 lysate made on the resulting strain. This allowed *ftsA*(*R286W*) to be cotransduced with *ftsQE14*::*kan* into the desired background (>90% linkage). To test suppression of Δ*ftsK*, we introduced a wild-type copy of FtsQ under control of the IPTG-inducible P_{206} promoter into the λ*att* site of JOE563. *ftsA*(WT), *ftsA*(*I143L*), or *ftsA*(*R286W*) was transduced into the resulting strain linked to *ftsQE14*::*kan*, and suppression was tested using glucose plus IPTG. To test suppression of Δ*zipA*, wild-type strain JOE309 was transformed with pBAD33-*ftsQ* and the temperature-sensitive, ZipA-expressing

TABLE 1. Strains and plasmids

Strain or plasmid	Relevant genetic marker(s) and/or features[a]	Source or reference
Strains		
KS272	F$^-$ Δ*lacX74 galE glaK thi rpsL* Δ*phoA*(PvuII)	Lab strain
MJC129	KS272 *ftsQ1*(Ts) *recA*::*cat*	24
JOE309	MC4100 *ara*$^+$	4
JOE417	JOE309 *ftsQE14*::*kan*/pBAD33-*ftsQ*	10
JOE424	KS272 *ftsQE14*::*kan*/pBAD33-*ftsQ*	J. Chen
NWG98	KS272 *ftsQE14*::*kan* Δ(λ*attL-lom*)::*bla lacI*^{q} P_{207}-*ftsQ*(*V254E*)/pBAD33-*ftsQ*	This study
NWG99	KS272 *ftsQE14*::*kan* Δ(λ*attL-lom*)::*bla lacI*^{q} P_{207}-*ftsQ*(*A252P*)/pBAD33-*ftsQ*	This study
NWG282	KS272 *ftsQE14*::*kan* Δ(λ*attL-lom*)::*bla araC* pBAD-*ftsQ*	This study
NWG283	KS272 *ftsQE14*::*kan* ϕ80*att*::P_{207}-*ftsL* Δ(λ*attL-lom*)::*bla araC*/*pBAD-ftsQ*	This study
NWG284	KS272 *ftsQE14*::*kan* ϕ80*att*::P_{207}-*ftsI* Δ(λ*attL-lom*)::*bla araC*/*pBAD-ftsQ*	This study
NWG453	JOE309 *ftsQE14*::*kan* ϕ80*att*::P_{207}-*ftsI*/pBAD33-*ftsQ*	This study
JOE100	MC4100 Δ(λ*attL-lom*)::*bla lacI*^{q} P_{207}-*gfp-ftsL leu*::Tn*10 ftsA12*(Ts)	18
NWG501	JOE309 Δ(λ*attL-lom*)::*bla lacI*^{q} P_{207}-*gfp-ftsB leu*::Tn*10 ftsA12*(Ts)	19
NWG531	JOE309 *ftsK-yfp* (Cam^r) *leu*::Tn*10 ftsA12*(Ts)	19
NWG706	JOE309 *ftsQE14*::*kan ftsA*(*I143L*) Δ(λ*attL-lom*)::*bla araC*/*pBAD-ftsQ*	This study
NWG707	JOE309 *ftsQE14*::*kan ftsA*(WT) Δ(λ*attL-lom*)::*bla araC*/*pBAD-ftsQ*	This study
NWG708	JOE309 *ftsQE14*::*kan ftsA*(*R286W*) Δ(λ*attL-lom*)::*bla araC*/*pBAD-ftsQ*	This study
Plasmids		
pTrc99a	IPTG-regulated P_{Trc} promoter, Ap^r	
pDSW204	IPTG-regulated P_{Trc} promoter, −35 down mutation, Ap^r	38
pDSW207	pDSW204-*gfp*-MCS (fusion vector)	38
pBAD18	P_{BAD} Ap^r (high copy number)	23
pBAD33	P_{BAD} Cm^r (medium copy number)	23
pBAD42	P_{BAD} Sp^r (low copy number, pSC)	L. M. Guzman
pJC2	pBAD18-*ftsN*	9
pJC85	pBAD42-*ftsK*	9
pGA4ΔBsp	MalF::PhoA	3
pNG1	pBAD18-*ftsQ-myc*	This study
pNG2	pBAD18-*ftsQ264-myc*	This study
pNG7	pBAD18-*ftsQ256-myc*	This study
pNG8	pBAD18-*ftsQ240-myc*	This study
pNG9	pBAD18-*ftsQ250-myc*	This study
pNG106	P_{tet}-*ftsQ*-3×-Myc	This study
pNG163	pSC (Sp^r) *lacI*^{q} P_{209}-*ftsQ*	This study
pNG153	pSC (Sp^r) *lacI*^{q} P_{204}-*zapA-QQQ*	19
pNG210	pDSW204-*ftsQ-myc3*	This study
pNG211	pDSW204-*ftsQ*(*L55P*)-*myc3*	This study
pNG212	pDSW204-*ftsQ*(*L60P*)-*myc3*	This study
pNG213	pDSW204-*ftsQ*(*V92D*)-*myc3*	This study
pNG214	pDSW204-*ftsQ*(*R196W*)-*myc3*	This study

[a] Ap^r, ampicillin resistance; Cm^r, chloramphenicol resistance; Sp^r, spectinomycin resistance.

plasmid pCH2. The resulting strain was then transduced with *ftsA*(WT), *ftsA*(*I143L*), or *ftsA*(*R286W*) linked to *ftsQE14*::Tn*10*. Finally, Δ*zipA*::*kan* from CH5 was linked to *nupC*::Tn*10* (34) and transduced into the strains carrying the various *ftsA* alleles. Following confirmation of the presence of the Δ*zipA*::*kan* allele, the strains were tested for suppression at 42°C.

Microscopy and image capture. For localization in FtsQ-depleted cells, an overnight culture was grown in NZ medium containing arabinose at 37°C. Cells were diluted, grown to the mid-log phase, and then diluted into NZ medium containing glucose and IPTG and grown until filamentation was obvious. Green fluorescent protein (GFP) fusions in the λ*att* site and pNG163 were induced with 10 μM and 2 μM IPTG, respectively. Premature targeting was performed as described by Goehring et al. (19). Briefly, log-phase cultures were shifted to 42°C for 65 min. GFP and ZapA fusions were induced with 20 μM IPTG for the final 30 min of growth. The efficiency of recruitment of a GFP fusion was quantified by measuring the average spacing of fluorescent GFP bands within a filamentous cell (ring spacing). Spacing of approximately 12 μm/ring or less was a positive recruitment score.

Cells were harvested, fixed (8), and mounted on agarose cushions for microscopy as described previously (37). In some cases, cells were stained with 0.2 μg/ml 4′,6-diamidino-2-phenylindole (DAPI) in phosphate-buffered saline and washed twice in phosphate-buffered saline before mounting. Cells were examined for fluorescence using an Axioskop 2 microscope (Zeiss) equipped with a 100× plan-Apochromat oil immersion objective and a 100-W mercury lamp. Filter sets to visualize enhanced GFP (HQ:FITC/Bodipy/Fluo3), enhanced yellow fluorescent protein, and DAPI (UV) were obtained from Chroma Technology Corp. Images were captured using an Orca-100 charge-coupled device camera (Hamamatsu Photonics) and Openlab (Improvision) and were subsequently processed and analyzed using Openlab. All measurements were limited to intact cells exhibiting normal nucleoid morphology. Final processing of images for presentation was performed using Adobe Photoshop.

Colony photography was performed in two ways. Routine images were captured using incident light with a Nikon D100 camera and a 60-mm Nikkor Macro lens (see Fig. 3E). To enhance the appearance of wrinkles, colonies were illuminated with a combination of incident light and transmitted light and visualized using a Stemi SV6 stereomicroscope (see Fig. 3A and B). Images were captured using an Axiocam charge-coupled device camera and Zeiss Axiovision 4.3 (Zeiss). In both cases, final processing was performed using Adobe Photoshop.

RESULTS

Characterization of a region of the FtsQ γ domain required for recruitment. A previous genetic study of *ftsQ* yielded a C-terminal truncation, FtsQ2, in which a stop codon replaced

TABLE 2. FtsQ γ domain mutants

Mutant	Colony morphology under the following conditions:		
	Glucose, 30°C	Arabinose, 30°C	Arabinose, 42°C
c-Myc truncations[a]			
None	Wrinkled[b]	Wrinkled	−
FtsQ2(Y249*)	Wrinkled	−[c]	−
FtsQ276-Myc (wild-type)	Wrinkled	+++	+++
FtsQ264-Myc	Wrinkled	+++	+++
FtsQ256-Myc	Wrinkled	+++	+++
FtsQ250-Myc	Wrinkled, small	−	−
FtsQ240-Myc	Wrinkled, small	−	−
PhoA fusions[d]			
FtsQ(WT)-PhoA	Wrinkled	+++	+++
FtsQ256-PhoA	Wrinkled	+++	++
FtsQ250-PhoA	Wrinkled	±	−
FtsQ240-PhoA	Wrinkled	±	−
FtsQ(V254E)-PhoA	Wrinkled	+++	−
FtsQ(A252P)-PhoA	Wrinkled	±	−

[a] All constructs were cloned under control of an arabinose-inducible promoter in pBAD18.
[b] An otherwise wild-type strain containing *ftsQ1*(Ts) formed wrinkled colonies and exhibited a slightly filamentous phenotype even at the permissive temperature.
[c] −, no growth; ±, poor growth; ++, slightly wrinkled colonies; +++, normal colony morphology.
[d] Alkaline phosphatase is fused in frame to the C terminus. The results for truncations with PhoA fusions are shown for comparison.

the Y248 codon (10). This mutant protein localized normally but did not recruit downstream proteins, providing the first demonstration that at least two functions of FtsQ (localization and recruitment) are genetically separable. Consistent with the FtsQ2 protein's ability to localize but not recruit, *ftsQ2* acted as a dominant negative to a temperature-sensitive allele of *ftsQ*, *ftsQ1*(Ts), at the permissive temperature.

We cloned five versions of FtsQ, four versions truncated at amino acids 240, 250, 256, and 264 and one full-length clone, all fused to a C-terminal c-Myc tag. We found that the *ftsQ240* and *ftsQ250* truncations did not complement *ftsQ1*(Ts) strain MJC129 at 42°C, whereas the remainder of the versions complemented this strain well (Table 2). Thus, amino acids 256 to 276 are dispensable for function. Similar to *ftsQ2*, *ftsQ240* and *ftsQ250* were also dominant negative to the *ftsQ1* allele at the permissive temperature, suggesting that FtsQ240 and FtsQ250 could outcompete FtsQ1 for localization to midcell and that amino acids 250 to 256 are critical for recruitment but not for localization. Notably, all truncations appeared to destabilize the protein when they were analyzed by Western blotting using antibodies to either FtsQ or c-Myc, and the effect increased with the size of the truncation (Fig. 2A and data not shown). FtsQ250 and FtsQ240 were barely detectable by Western blotting. Perhaps not surprisingly given this result, neither FtsQ240 nor FtsQ250 acted as a dominant negative in a wild-type background.

We next tried to generate a point mutation that resulted in a phenotype similar to that of the truncation mutants, yet encoded a more stable protein. To this end, we used plasmid pNG17, which encoded an FtsQ::PhoA fusion carrying restriction sites flanking amino acids 250 to 256. The C-terminal alkaline phosphatase (PhoA) fusion was included to allow ready elimination of carboxy-terminal truncation mutants that could be detected by the loss of alkaline phosphatase activity. We screened mutagenized plasmid pools in which codons 251 to 256 were scrambled by testing for complementation of the *ftsQ1*(Ts)-containing strain MJC129. Transformants were screened on NZ medium containing arabinose and 5-bromo-4-chloro-3-indolylphosphate (XP) at permissive (30°C) and nonpermissive (42°C) temperatures. Several colonies had the desired phenotype; they were blue on XP-containing plates (they retained PhoA activity) and did not grow at 42°C. Several mutants also produced small blue colonies at 30°C, indicative of a potential dominant negative phenotype. Candidate mutants were then tested for expression by Western blotting (Fig. 2A). Mutant proteins that were expressed at a level that was at least 60% of the level of the wild-type FtsQ-PhoA fusion were sequenced, and the following two candidates were chosen for further characterization: FtsQ(A252P) and FtsQ(V254E). The phenotypes of these mutants are shown along with those of the truncation alleles in Table 2. Notably, when fused to PhoA, FtsQ250 was produced at a level significantly higher than that of endogenous FtsQ due to stabilization by alkaline phosphatase (data not shown). Thus, the phenotype of this truncation is not due to reduced protein levels, as could have been suggested by the instability of the c-Myc-tagged version.

To study localization, the two mutants were subcloned into the GFP fusion vector pDSW207, and a single copy was integrated into the chromosome of an FtsQ depletion strain

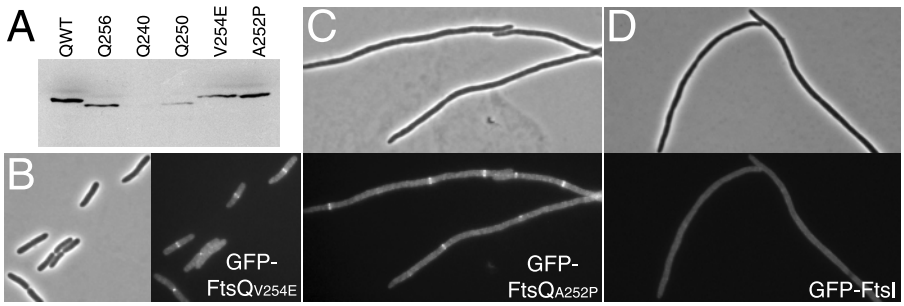

FIG. 2. Analysis of C-terminal mutations in FtsQ affecting recruitment of downstream proteins. (A) Western blot of C-terminal truncations and point mutations fused to *phoA*. (B and C) Localization of GFP-FtsQ(V254E) and GFP-FtsQ(A252P) in an FtsQ depletion strain, respectively. (D) Recruitment of GFP-FtsI by FtsQ(A252P) in an FtsQ depletion strain. Phase-contrast and GFP channels are shown. Recruitment of GFP-FtsI by wild-type FtsQ is shown in Fig. S1in the supplemental material, which was obtained in parallel with the image shown in panel D.

(JOE424) in which FtsQ was expressed from pBAD33 (10). This FtsQ depletion strain required arabinose for growth. The resulting strains expressing the FtsQ mutants, NWG98 (V254E) and NWG99 (A252P), were grown on glucose media to repress wild-type FtsQ expression, and expression of the GFP fusions to the mutant proteins was induced with 10 μM IPTG in order to test for complementation and localization. Surprisingly, NWG98 grew well on glucose, forming slightly elongated cells (average length, 10.4 μm). The GFP-FtsQ(V254E) fusion also localized to the midcell of most cells (25/29 cells) despite being present at significantly lower levels than the control GFP-FtsQ fusion (Fig. 2B). Given its weak phenotype, we did not examine this mutant further. In contrast, NWG99 grew as long filaments, indicating that FtsQ(A252P) still did not complement when it was fused to GFP (average length, 51.2 μm). Nonetheless, GFP-FtsQ(A252P) was present at amounts similar to the amounts of the control GFP-FtsQ and localized normally to potential division sites along the length of the filaments (Fig. 2C).

In order to assess recruitment of downstream proteins by FtsQ(A252P), we removed the GFP tag and expressed FtsQ(A252P) independent of both IPTG (required for expression of GFP fusions to other division proteins) and arabinose (required for complementing the copy of FtsQ in the depletion strain). For these purposes, we created a plasmid, pNG106, in which an *ftsQ* allele containing a C-terminal 3×-Myc tag was placed under control of a pTET promoter. When the plasmid was introduced into an FtsQ depletion strain, basal expression of FtsQ from the plasmid complemented for growth and resulted in FtsQ levels that were approximately fivefold greater than the endogenous FtsQ levels (data not shown). FtsQ(A252P) was subcloned into pNG106 and introduced into FtsQ depletion strains NWG283 and NWG284. These strains were similar to the strain described above, except that the pBAD-regulated *ftsQ* allele was on the chromosome and they expressed GFP fusions to FtsL (NWG283) and FtsI (NWG284). The resulting strains were grown in media containing glucose, and IPTG was added to induce the GFP fusions. No localization of FtsL or FtsI was seen, indicating that the mutant, although it localized normally, was unable to recruit downstream proteins (Fig. 2D and data not shown). Despite these characteristics, FtsQ(A252P) was not dominant negative in a wild-type background. The finding that FtsQ (A252P) and the FtsQ truncations were dominant only in an *ftsQ1* (Ts) background suggested that these mutant proteins could not compete with FtsQ(WT) for binding sites at the division site. Such a defect could have been due either to a minor inherent localization defect or to the loss of cooperative localization signals resulting from the association of FtsQ with downstream division proteins.

Wrinkled-colony-based screen for identification of nonlethal *fts* mutants. In our genetic studies of FtsQ (10; this study) we have focused primarily on identifying highly defective mutant alleles of *ftsQ*. Screens have been performed using high levels of FtsQ expression (>10× endogenous FtsQ levels) and have been focused on finding alleles that cannot complement the *ftsQ1*(Ts) allele at the restrictive temperature. The majority of the mutant alleles isolated by these screens appeared to encode unstable proteins (they did not produce significant quantities of protein, as measured by Western blotting), and many were found to contain multiple mutations. Finding a point mutation that disrupted function in such a screen required targeted and saturating mutagenesis of a defined region (see above). These observations suggested that single amino acid changes that can completely eliminate an essential activity of FtsQ but do not destabilize the protein are relatively rare or, for some activities, such as localization, may not exist. We reasoned that a screen for FtsQ point mutants that exhibited more moderate growth defects would allow us to isolate novel alleles of FtsQ, which we hoped would be informative regarding the regions of FtsQ involved in localization, recruitment, and function.

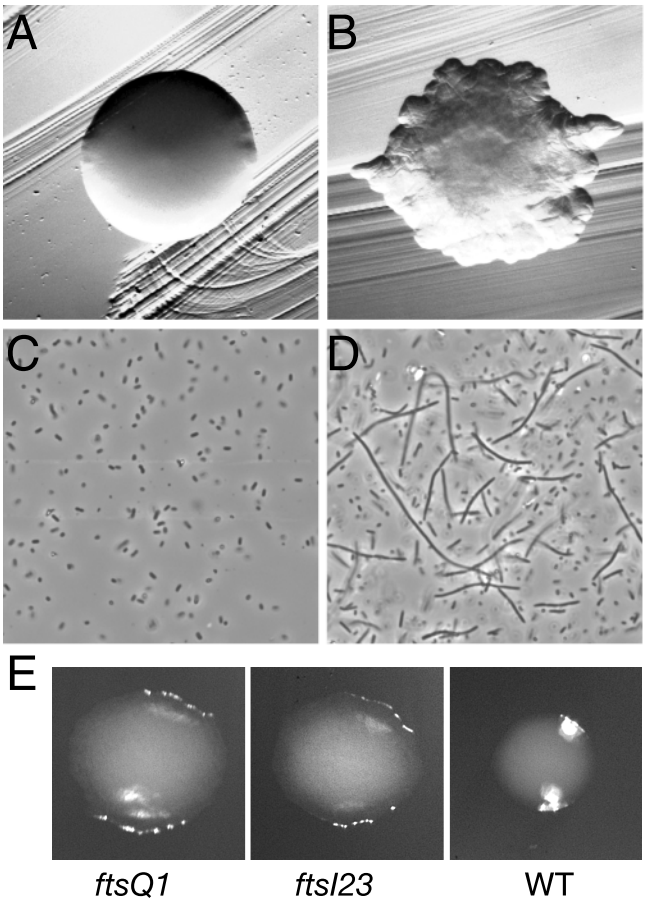

FIG. 3. Leaky cell division mutants lead to a wrinkled-colony morphology, which reflects growth as elongated cells and filaments. (A) Colony formed by the FtsB depletion strain NB946 grown on M63 medium containing arabinose to induce expression of FtsB. (B) Colony formed by the same strain on M63 medium containing glucose (FtsB expression was repressed). (C and D) Phase-contrast images of cells isolated from colonies shown in panels A and B, respectively. (E) Colonies formed by a wild-type strain (WT) and isogenic strains carrying either the *ftsQ1*(Ts) or *ftsI23*(Ts) allele grown at 30°C, the permissive temperature for these mutations. Note the uneven flattened (spreading) edge around the temperature-sensitive colonies compared to the wild-type colony. The imaging methods used are described in Materials and Methods.

In the course of identifying conditions for such a screen, we noticed a rather peculiar characteristic of an FtsB depletion strain (NB946). On rich media, this strain grew normally when arabinose was present (in this medium the complementing copy was induced), but it did not grow when another sugar, such as glucose, was used (in this medium the complementing copy was repressed). However, on M63 medium containing

TABLE 3. Characterization of wrinkled-colony mutants

Allele	Wild-type fraction with rings[a]	Δ*ftsQ*		Localization of FtsI: ring spacing (μm/ring)[d]	Ring spacing forrecruitment by ZapA fusion (μm/ring)[e]		
		Ring spacing (μm/ring)[b]	Cell length (μm)[c]		FtsK	FtsL	FtsB
None	NA[g]	NA	47.0	214.8	25.0 (17)	39.8 (18)	20.1 (8)
Wild type	0.56	7.4	4.0	8.2	**6.8** (30)	**8.1** (25)	**6.8** (23)
A252P[f]	ND	11.2	51.2	−	**6.8** (16)	56.1 (14)	292 (16)
L55P	0.67	9.3	10.9	17.5	**7.3** (25)	**8.2** (21)	**8.2** (9)
L60P	0.05	609.4	13.9	50.7	**10.5** (36)	**9.2** (29)	**8.8** (24)
V92D	0.17	49.0	15.9	21.9	**7.4** (38)	**7.2** (21)	**7.5** (23)
R196W	0.56	12.3	18.8	18.6	**6.5** (30)	**8.5** (33)	**9.7** (30)

[a] Fraction of cells expressing a GFP fusion to the *ftsQ* allele that have a fluorescent band at midcell.
[b] Average spacing of fluorescent bands at putative division sites exhibited by FtsQ-depleted cells (NWG282) expressing GFP fusions to *ftsQ* alleles.
[c] Average cell length for FtsQ-depleted cells complemented by GFP fusions to *ftsQ* alleles.
[d] Localization of FtsI in FtsQ-depleted cells expressing untagged *ftsQ* alleles from the λ*att* site with 10 μM IPTG (λ*att*::P_{204}-*ftsQ*). The average spacing of GFP-FtsI rings in the resulting cells reflects the ability of the *ftsQ* allele to promote localization of downstream cell division proteins.
[e] Recruitment by ZapA-FtsQ allele fusions in an *ftsA12*(Ts) background as determined by a premature targeting assay. FtsQ mutants were fused to ZapA, and recruitment of the GFP fusions was quantified by measuring ring spacing. Previous work suggested that a ring spacing of approximately 10 μm/ring is a positive recruitment score; values of approximately 10 μm/ring are indicated by boldface type. For details see Materials and Methods and reference 19. The numbers of cells quantified are indicated in parentheses.
[f] Data for A252P (obtained from experiments whose results are shown in Fig. 2) are shown for comparison. ND, not done; −, no localization of the GFP fusion analyzed.
[g] NA, not applicable.

glucose, expression was not induced, but the strain was nonetheless able to grow, albeit with a significant defect in colony morphology. The colonies appeared to be wrinkled, with rough edges (Fig. 3B). Inspection of the cells in the colonies revealed that there was a large proportion of filamentous cells, indicating that division was not normal (Fig. 3D). Growth required the presence of the complementing copy of the gene, indicating that basal levels of expression from the pBAD promoter provided some ability to divide, if the growth rate was low enough. A similar wrinkled morphology was observed for strains carrying certain *fts* mutations (*ftsK44*, *ftsI23*, *ftsQ1*), presumably due to partial defects at the permissive temperature (Fig. 3E). In what is likely a related phenomenon, a transposon screen with cyanobacteria yielded colonies with an "extensively spreading" phenotype, two of which exhibited cell division defects. One insertion turned out to disrupt the gene encoding an FtsZ-binding protein, ZipN (27). Thus, the wrinkled-colony morphology appears to be a general phenotype of leaky mutants with mutations in cell division proteins, and it provided the desired basis for our screen.

To seek mutant alleles of FtsQ with the wrinkled-colony approach, we used plasmid pNG106. As described above, the level of expression of FtsQ from this plasmid is low but sufficient for normal growth. This plasmid was also compatible with the FtsI recruitment test strain (NWG284), which allowed rapid determination of the ability of FtsQ mutant proteins to recruit FtsI. We were particularly interested in mutants that supported localization of downstream proteins, as such mutants would be predicted also to localize and thus would presumably be defective in a previously unidentified FtsQ activity.

The *ftsQ* coding sequence was subjected to PCR mutagenesis and ligated into pNG106. Pools of mutagenized plasmid were transformed into the tester strain NWG284. Following transformation, the cells were plated on NZ medium containing glucose to repress the complementing (pBAD-regulated) *ftsQ* allele. Colonies having a wrinkled morphology were restreaked on the same medium to confirm the phenotype before they were returned to arabinose-containing medium. The resulting wrinkled-colony mutants were then grown in liquid NZ medium containing glucose to determine for each mutant the magnitude of the division defect, the relative level of protein, and the ability to recruit FtsI. On the basis of these assays, we selected the following four mutants for further characterization: L55P, L60P, V92D, and R196W. All four mutants produced detectable amounts of FtsQ, as measured by Western blotting (data not shown), and exhibited some FtsI localization upon initial inspection (see Fig. S1 in the supplemental material; data not shown).

Functional characterization of wrinkled-colony *ftsQ* mutants. In order to more fully characterize the selected mutants, we subjected them to a variety of standard assays, including analyses confirming their ability to recruit downstream proteins, measuring their ability to localize to midcell, and testing their associations with upstream and downstream proteins using our recently developed premature targeting assay. The results obtained are shown in Table 3.

We initially wanted to confirm the ability of these mutants to recruit downstream proteins because expression of the mutants from plasmid pNG106 resulted in high cell-to-cell variation in the FtsI localization signal. To eliminate this variation, which could have been due to both the promoter used and stochastic variations in plasmid copy number, we repeated our recruitment analysis using chromosomally integrated constructs under control of the IPTG-inducible P_{204} promoter. When GFP-FtsI and the FtsQ mutants were induced with 10 μM IPTG, we found that all four mutants exhibited defects in FtsI localization compared to the wild-type control.

We then determined whether the defects associated with the mutants were due to inefficient localization to midcell. To do this, the mutations were introduced into pNG163, a low-copy-number plasmid expressing a GFP fusion to FtsQ under control of the P_{206} promoter. The abilities of the mutants to localize were then analyzed both in a wild-type strain, JOE309, and in an FtsQ depletion strain, NWG282. L60P and V92D

TABLE 4. Effects of replacing the transmembrane anchor of $FtsQ_{V92D}$ on growth, localization, and suppression by alleles of *ftsA*

ftsQ allele	Phenotype of *ftsQ* alleles in Δ*ftsQ ftsA* (wild-type/suppressor) backgrounds[a]									
	ftsA phenotype (chromosome)[b]	*ftsA*(WT)			*ftsA*(*I143L*)			ftsA(*R286W*)		
		Phenotype (plasmid)	Ring spacing (μm/ring)	Cell length (μm)	Phenotype (plasmid)	Ring spacing (μm/ring)	Cell length (μm)	Phenotype (plasmid)	Ring spacing (μm/ring)	Cell length (μm)
ftsQ(WT)	+++	++	8.3	3.9	+++	4.2	3.3	+++	4.7	3.5
ftsQ(*V92D*)	wr	WR[c]	16.8	14.8	++[c]	7.5	6.2	++[c]	8.0	5.6
FFQ(WT)	+++	++	12.2	3.6	+++	5.5	3.2	++	7.7	3.2
FFQ(*V92D*)	−	−	232.1	51.6	wr[c]	47.6	14.1	WR[c]	89.5	24.9

[a] All strains are Δ*ftsQE14*::*kan* complemented by pBAD-*ftsQ*. See Table 1 for details. Phenotype (plasmid) is colony morphology of FtsQ depletion strains under depletion conditions carrying various *ftsA* alleles [*ftsA*(WT), NWG707; *ftsA*(*I143L*), NWG706; *ftsA*(*R286W*), NWG708] and complemented by GFP-tagged *ftsQ* alleles expressed from the low-copy-number plasmid pNG163. Ring spacing is determined as total length of cells examined/total number of fluorescent rings at potential division sites. Cell length is the average cell length of cells examined and reflects ability of each GFP fusion to support cell division in the indicated *ftsA* background. +++, normal growth; ++, slightly wrinkled; wr, wrinkled; WR, extensively wrinkled; −, no growth.

[b] Colony morphology of an FtsQ depletion strain (JOE417) under depletion conditions complemented by untagged *ftsQ* alleles expressed as a single copy from a weak promoter (λ*att*::pDSW206).

[c] Representative colonies for the indicated conditions are shown in Figure 7 and provide examples of the indicated plate phenotypes.

exhibited localization defects in both wild-type strain JOE309 and FtsQ depletion strain NWG282. In contrast, L55P and R196W exhibited nearly wild-type levels of localization. Western blotting confirmed that GFP fusions to all four mutants were produced at equivalent protein levels and primarily as full-length fusion proteins, indicating that the localization defects were due neither to cleavage of GFP nor to lower protein levels (data not shown).

Finally, to assess the abilities of the mutants to associate in vivo with upstream and downstream cell division proteins, the mutants were analyzed using the recently developed premature targeting technique (21). In this method, a protein is fused to the FtsZ binding protein ZapA, which allows it to be targeted directly to FtsZ. In otherwise wild-type cells, when FtsA is depleted, FtsK, FtsL, FtsB, FtsW, FtsI, and FtsN are not localized to midcell. When the ZapA-FtsQ(WT) fusion is expressed under these conditions, it restores localization of FtsK, FtsL, FtsB, FtsW, and FtsI. This recruitment reflects the ability of ZapA-FtsQ(WT) to interact with and recruit upstream and downstream proteins independent of FtsA. Failure of FtsQ mutants to behave similarly would indicate defects in particular associations. This approach should be particularly useful for analyzing mutant proteins that may be defective for localization, as this method of assessing recruitment does not require that the protein is able to localize on its own.

We first performed this analysis with FtsQ(A252P). A ZapA-FtsQ(A252P) fusion did not restore localization of FtsL and FtsB, reflecting its defect in recruitment, yet it was able to restore localization of FtsK, consistent with its ability to localize in an otherwise wild-type background. In contrast, all wrinkled-colony mutants restored localization of FtsK, FtsL, and FtsB, suggesting that they were not completely defective in any of these interactions. This finding is perhaps not surprising since all four "wrinkled-colony" mutants were only partially defective for cell division.

Nonessential membrane anchor of FtsQ is essential in FtsQ(V92D). Previous results of a "swap" analysis of FtsQ showed that the polypeptide sequence of the cytoplasmic and transmembrane domains of FtsQ is not essential (12, 24) and that the role of this region may be mainly to tether the protein to the membrane. In these experiments, the amino-terminal membrane anchor of MalF or MalG could be substituted for the cytoplasmic and transmembrane segments of FtsQ without causing a loss of function. Recent work by Geissler et al., on the other hand, suggested that this amino-terminal region of FtsQ contributes to divisome stability; it was required for the ability of FtsQ, when overexpressed, to rescue a Δ*ftsK* strain (16). A GFP fusion to FFQ, an FtsQ swap construct in which the cytoplasmic and transmembrane segments of FtsQ were replaced by the corresponding domains from MalF, showed a mild localization defect (24) (Table 4). Thus, we wondered whether a potential contribution by this region of FtsQ to localization masked the severity of the disruption between the divisome and FtsQ caused by our localization mutants. Evidence for such an effect would indicate a role for the amino-terminal region of FtsQ in the targeting of the protein to division sites.

To test for a modulating role of amino acids 1 to 49 of FtsQ in the behavior of our localization mutants, we compared FtsQ(V92D), full-length FtsQ(WT), an otherwise wild-type swap construct [FFQ(WT)], and a swap construct containing the V92D mutation [FFQ(V92D)]. These constructs were placed under control of an IPTG-inducible promoter (P_{206}), single copies were integrated at the λ*att* site in an FtsQ depletion strain, and complementation was assessed. All of the constructs produced nearly equivalent amounts of protein (data not shown). As expected, when induced with IPTG, FtsQ(WT) and FFQ(WT) both complemented the FtsQ depletion strain. FtsQ(V92D) also complemented well for colony formation, but it had the expected wrinkled-colony phenotype. Strikingly, the swap construct containing the V92D mutation [FFQ (V92D)] failed to complement at all (λ*att*::P_{206}) (Table 4). We observed the same effect with FQQ, in which only the cytoplasmic domain was swapped (data not shown), indicating that the amino-terminal region, specifically including at least some portion of the cytoplasmic domain, is important for optimal FtsQ function.

We then asked whether the lack of complementation of FFQ(V92D) was due to enhancement of the localization defect caused by the V92D lesion. To examine this possibility, we fused each construct to GFP in plasmid pNG163. The addition of GFP to the N terminus slightly exacerbated the defects of

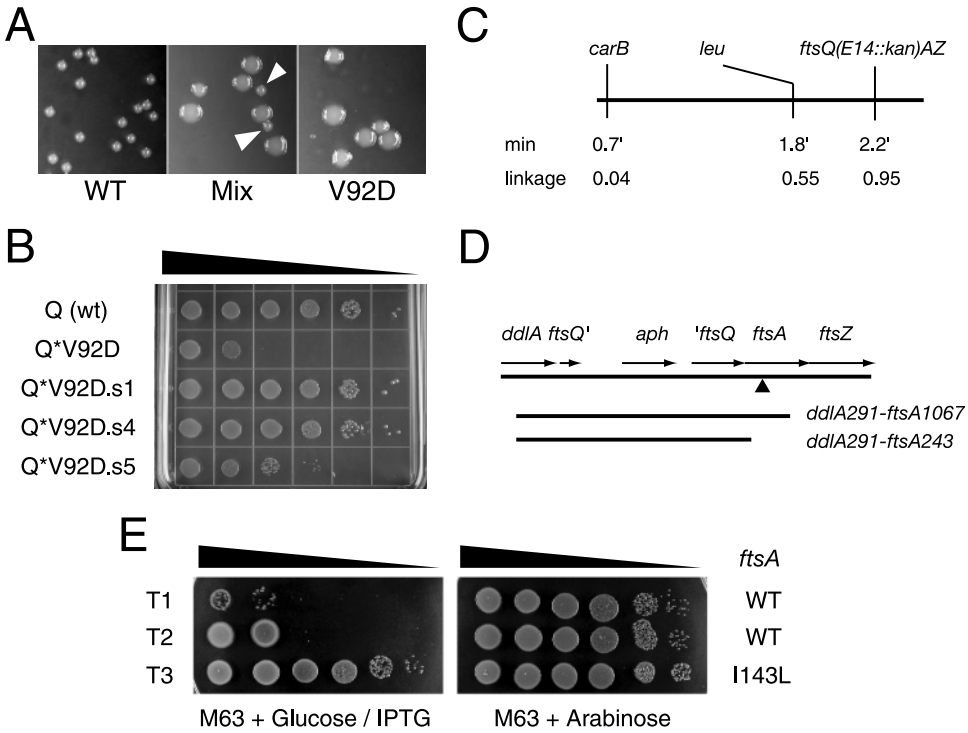

FIG. 4. Suppressor analysis of FtsQ(V92D). (A) Comparison of the wild type (WT) and the FtsQ(V92D) wrinkled-colony mutant on NZ medium. Arrowheads indicate wild-type colonies. (B) Relative CFU from overnight cultures of Δ*ftsQ* cells expressing wild-type FtsQ [Q (wt)] or FtsQ(V92D) (Q*V92D). Equivalent dilutions (standardized using optical density at 600 nm) were plated on M63 medium containing glucose and 20 μg/ml kanamycin plus 1 mM IPTG. Putative suppressors of FtsQ(V92D) are designated Q*V92D.s1, Q*V92D.s4, and Q*V92D.s5. (C) Map of the 2-minute region of the *E. coli* chromosome with linkage of suppressor FtsQ*(V92D).s1 to the markers indicated. (D) Position of the *ftsA*(*I143L*) mutation in the chromosome, indicated by the solid triangle. The position of the *ftsQE14*::*kan* allele is indicated. The linear PCR products used to confirm the sufficiency of the *ftsA*(*I143L*) suppressor are indicated at the bottom. (E) Plating efficiencies of three independent transformants of the *ddlA291-ftsA1067* PCR product. T1 and T2 did not show suppression on M63 medium and were wild type for *ftsA*. T3 showed suppression and contained the I143L mutation. Plating efficiency was tested as described above for panel B. Plating on M63 medium containing arabinose (wild-type FtsQ expressed from pBAD33) served as a control for plating efficiency.

the various constructs when they were analyzed on plates (pNG163) (Table 4). The pattern, however, was the same as the pattern for the untagged constructs. We then compared the abilities of the various FtsQ constructs to localize in cells in which wild-type FtsQ was depleted. Strikingly, the GFP fusion to FFQ(V92D) showed a nearly complete failure to localize. By contrast, GFP fusions to FtsQ(V92D) and FFQ localized somewhat better, although they localized less efficiently than a fusion to FtsQ(WT) localized. These experiments also confirmed the decreased ability of FFQ(V92D) to complement, which was reflected by the increase in the average cell length of FFQ(V92D)-expressing cells compared to cells expressing the other FtsQ constructs. Thus, although the first 49 amino acids comprising the cytoplasmic and transmembrane domains are not required for targeting of FtsQ to midcell, they contribute to the affinity of FtsQ for upstream divisomal components.

Suppressor analysis of FtsQ(V92D). Based on its reduced ability to localize, we concluded that the V92D mutation disrupts an interaction between FtsQ and upstream division proteins. As such, suppressors should provide information about the nature of this disruption as one would expect compensatory changes in the interacting partners to rescue FtsQ(V92D).

For isolation of suppressor mutations, we created two strains in which either *ftsQ*(WT) or *ftsQ**(*V92D*) was expressed under control of a P_{206} promoter from the λ*att* site and in which the native *ftsQ* gene was deleted. Both strains required 100 μM to 1 mM IPTG for normal growth. However, whereas the strain carrying wild-type *ftsQ* formed smooth colonies when it was induced with 1 mM IPTG, the strain carrying *ftsQ**(*V92D*) formed large wrinkled colonies (Fig. 4A). We tried to identify conditions that allowed us to readily isolate suppressors of *ftsQ*(*V92D*). When we compared the plating efficiencies of the two strains on a variety of media, we found that on M63 medium containing glucose and 20 μg/ml kanamycin plus 1 mM IPTG, the strain expressing *ftsQ*(*V92D*) formed colonies at a frequency of approximately 10^{-4} to 10^{-5} relative to a strain expressing *ftsQ*(*WT*) (Fig. 4B). When colonies that did appear were picked and retested on the same medium, several of them had a smoother-colony phenotype and exhibited levels of plating efficiency that were nearly wild-type levels, indicating that they likely contained revertants or suppressor mutations (Fig. 4B). PCR analysis confirmed that no significant chromosomal rearrangements had occurred near the *ftsQE14*::*kan* allele in any of the potential suppressors (data not shown).

Several potential suppressors were then analyzed for linkage to known cell division proteins by testing for loss of suppression upon transduction of a linked marker. Two suppressors, *ftsQ*(*V92D*).*s1* and *ftsQ*(*V92D*).*s4*, showed linkage to the *mraY*

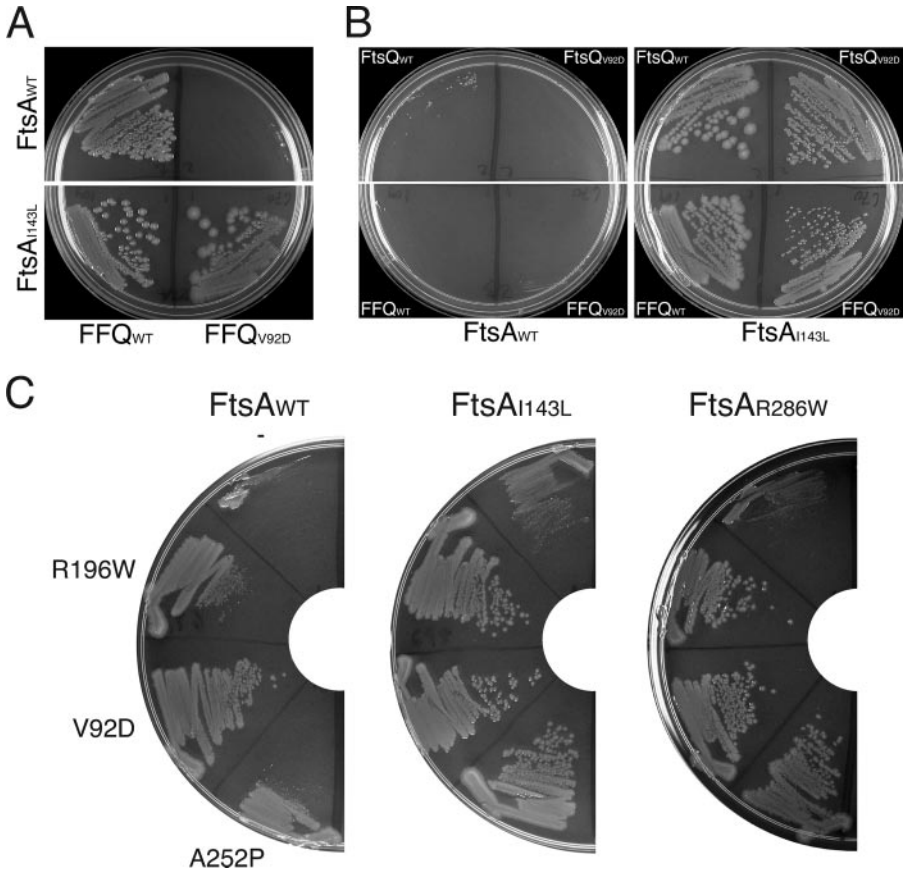

FIG. 5. (A) FtsA(I143L) acted as a general suppressor of FtsQ defects. *ftsA*(*I143L*) suppressed an FFQ(V92D) construct that was normally unable to complement growth of a Δ*ftsQ* strain. (B) FFQ and FFQ(V92D) were induced with 1 mM IPTG, and *ftsA*(*I143L*) permitted growth of strains expressing insufficient FtsQ to permit growth. All *ftsQ* alleles were uninduced. (C) Rescue of the recruitment-defective R196W and A252P alleles was performed as described for panel A.

gene cluster, which contains a large proportion of the genes involved in cell division and cell wall synthesis. These suppressors were mapped further using two additional markers in the region, *carB*::Tn*10* and Δ*ftsQE14*::*kan*. Only *ftsQ*(*V92D*).*s1* showed linkage to both markers (Fig. 4C). Sequencing of the *ftsQAZ* operon from this strain revealed two point mutations in *ftsA*. One was silent (Q340; CAG → CAA), while the other resulted in an isoleucine-to-leucine change at position 143 (I143L; ATC → CTC).

To confirm that *ftsA*(*I143L*) was sufficient to suppress *ftsQ*(*V92D*), we initially cloned *ftsA*(*I143L*) into pBAD33 and tested suppression. However, due to the detrimental effects of FtsA overexpression, we were unable to proceed with this strategy. Instead, we introduced the mutation directly into the chromosome using a linear PCR product. After isolating chromosomal DNA from the *ftsQ*(*V92D*).*s1* suppressor, we generated linear PCR products encompassing the C terminus of *ddl*, the *ftsQE14*::*kan* insertion, and various amounts of the *ftsA* gene (*ddlA291-ftsA1067* or *ddlA291-ftsA243* [Fig. 4D]). When the PCR product was transformed into a wild-type strain expressing *ftsQ**(*V92D*) at the λ*att* site, suppressed isolates were recovered at a high frequency (two of seven isolates tested) among Kan^r (*ftsQE14*::*kan*) recombinants, provided that the I143L mutation was present in the PCR product (only *ddlA291-ftsA1067*). Sequencing of a suppressed isolate confirmed the presence of the I143L mutation, while unsuppressed recombinants had the wild-type sequence (Fig. 4E). Sequencing of the linear PCR products revealed no mutations other than *ftsA*(*I143L*). Thus, the I143L mutation was solely responsible for suppression.

Characterization of FtsA(I143L) as a general suppressor of FtsQ defects. Given that FtsQ(V92D) had a defect in localization, one explanation of suppression was that FtsA(I143L) restored the localization of FtsQ(V92D). As shown in Table 4, *ftsA*(*I143L*) restored localization of a GFP fusion to FtsQ(V92D) to levels similar to the level of FtsQ(WT) in an *ftsA*(WT) background. In fact, compared to *ftsA*(WT), *ftsA*(*I143L*) also increased the localization efficiency of GFP-FtsQ(WT). The latter result was most likely due to a subtle localization defect in the wild-type protein caused by the N-terminal GFP moiety, a defect that was suppressed by FtsA(I143L). However, regardless of the ultimate mechanism, these results demonstrated that the I143L mutation in FtsA promoted FtsQ localization.

The simplest mechanism by which FtsA(I143L) could promote localization of FtsQ(V92D) was strengthening of a direct interaction between the two proteins. Such an interaction has been detected by two bacterial two-hybrid assays (14, 25). Rescue, however, could not be due to a simple compensatory

change in FtsA to accommodate the V92D lesion in FtsQ; the V92D change is in the FtsQ periplasmic domain, and FtsA is a cytoplasmic protein. To explain this paradox, one might postulate that FtsA binds the cytoplasmic tail or membrane anchor of FtsQ, increasing the affinity of the membrane anchor for the divisome and thereby compensating for the decreased affinity of the periplasmic domain of FtsQ for the divisome. This model makes the straightforward prediction that the membrane anchor of FtsQ is required for suppression. Thus, FtsA(I143L) should have been unable to suppress the defects of the FFQ(V92D) swap construct (described above) in which the membrane anchor was replaced with the 5′ cytoplasmic tail and the first transmembrane segment of the unrelated protein MalF.

As noted above, although FFQ efficiently complemented an FtsQ depletion strain, FFQ(V92D) was unable to complement. However, when introduced into an FtsQ depletion strain containing the FtsA(I143L) suppressor mutation, FFQ(V92D) was able to complement, although only wrinkled colonies were formed (Fig. 5A). Moreover, FtsA(I143L) also promoted the increased localization of GFP fusions to both FFQ(WT) and FFQ(V92D) compared to FtsA(WT) (Table 4). Thus, the I143L mutation could not strengthen a direct interaction between FtsA and FtsQ.

In the course of this experiment, we noticed that FtsA(I143L) also reduced the amount of FtsQ in cells that was required for growth. Normally, when single copies of our FtsQ constructs [FtsQ, FFQ FtsQ(V92D), FFQ(V92D)] were present, expression had to be induced to allow complementation. If IPTG was omitted, none of these constructs complemented an FtsQ depletion strain (Fig. 5B). Strikingly, introduction of *ftsA*(*I143L*) into these strains allowed growth on media lacking IPTG. *ftsA*(*I143L*) did not, however, rescue growth of the FtsQ depletion strain alone (data not shown), indicating that basal expression of FtsQ from the λ*att* constructs was required, and hence the suppressor did not entirely eliminate the need for FtsQ.

Given the general nature of the suppressor phenotype, we next tested whether *ftsA*(*I143L*) could suppress other lesions of *ftsQ*. If FtsA(I143L) only promoted the localization of FtsQ, it should have been unable to rescue mutants such as FtsQ(R196W) and FtsQ(A252P), both of which showed no localization defect. However, when we introduced these alleles into FtsQ depletion strains that contained either wild type *ftsA* or the *ftsA*(*I143L*) allele, we found that both alleles were rescued to some degree by *ftsA*(*I143L*) (Fig. 5C).

I143L and R286W mutations in FtsA result in similar but distinct phenotypes. Given its ability to suppress a variety of defects in FtsQ, we asked whether *ftsA*(*I143L*) also was able to suppress a variety of other division defects. In fact, a suppressor in *ftsA* with just such abilities was recently described. The allele, *ftsA*(*R286W*) (also known as *ftsA**), was isolated in a search for suppressor mutations that could eliminate the requirement for the essential protein ZipA (15). *ftsA*(*R286W*) was also able to rescue several other division defects, including deletion of *ftsK* and the *ftsQ1*(Ts) allele. To determine whether the two alleles acted in a similar manner, we directly compared the abilities of the two *ftsA* alleles to rescue deletion alleles of *ftsK* and *zipA*, as well as our newly isolated mutant alleles of *ftsQ*.

We first introduced the *ftsA* alleles into a strain in which the chromosomal copy of *ftsK* was deleted and growth was complemented by expression from a P_{BAD} promoter. While an isogenic strain carrying *ftsA*(WT) failed to grow when FtsK expression was repressed, both strains carrying *ftsA* suppressor mutations grew well (Fig. 6A). To test suppression of Δ*zipA*, we introduced the *ftsA* alleles into a strain in which the only copy of *zipA* was present on a plasmid with a temperature-sensitive replicon. At 42°C, this strain (containing wild-type *ftsA*) did not grow. However, when either *ftsA* suppressor was introduced, growth was rescued. *ftsA*(*R286W*) suppressed somewhat better than *ftsA*(*I143L*), allowing formation of significantly larger colonies (Fig. 6B). Finally, we compared the abilities of the *ftsA* alleles to suppress mutations in FtsQ. Both alleles were capable of suppressing the V92D, R196W, and A252P alleles to some degree (Fig. 5C). However, when we used a viability assay to test suppression of V92D in particular,

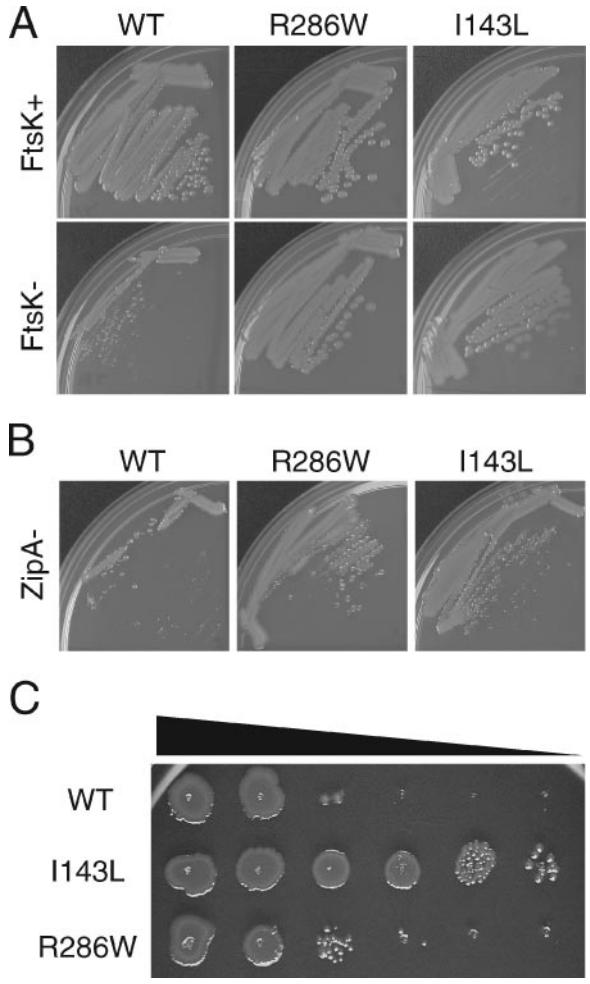

FIG. 6. Comparison of I143L and R286W mutations in FtsA. (A) Suppression of a FtsK depletion strain. FtsK+ and FtsK− indicate induction (arabinose) or repression (glucose) of the complementing copy of FtsK. (B) Suppression of a Δ*zipA* deletion upon loss of the complementing temperature-sensitive plasmid. (C) Suppression of FtsQ(V92D). Equal dilutions of cultures (standardized using optical density at 600 nm) containing cells expressing FtsQ(V92D) and the different *ftsA* alleles were plated on M63 medium containing glucose and 20 μg/ml kanamycin plus 1 mM IPTG. WT, wild type.

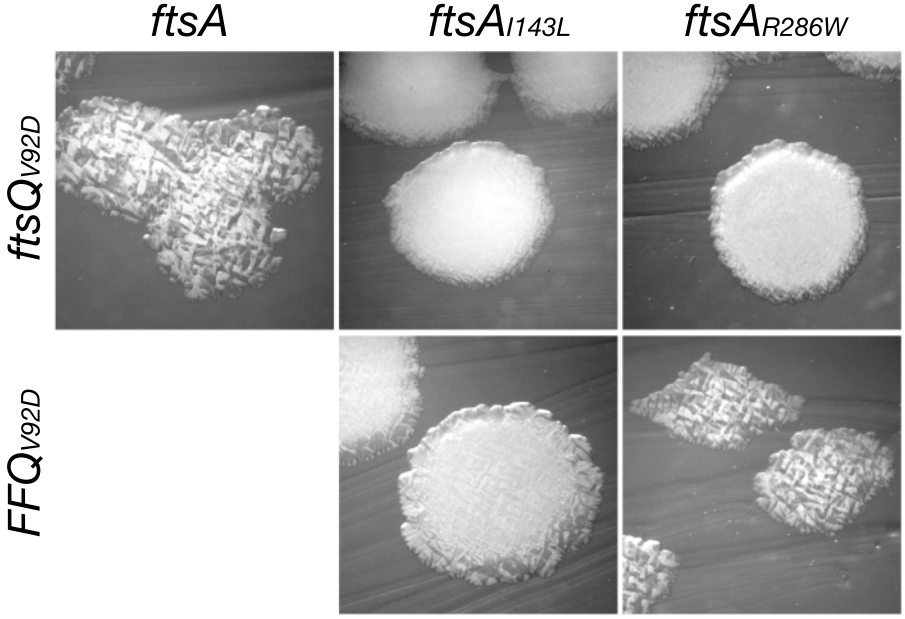

FIG. 7. Morphology of colonies expressing GFP fusions to FtsQ(V92D) and FFQ(V92D) in *ftsA* and *ftsA** backgrounds. FtsQ depletion strains containing different alleles of FtsA (NWG706, NWG707, and NWG708) were transformed with pNG163 containing GFP fusions to either FtsQ(V92D) or FFQ(V92D). The resulting strains were streaked on NZ medium containing glucose to repress the complementing wild-type copy of *ftsQ* and were allowed to grow overnight at 37°C.

FtsA(I143L) appeared to be a better suppressor (Fig. 6C). Despite this difference, we found that *ftsA*(*R286W*) was also able to restore localization of a GFP fusion to FtsQ(V92D) in FtsQ-depleted cells grown in liquid culture (Table 4). However, compared to FtsA(I143L), FtsA(R286W) was less able to suppress the localization defects associated with FFQ(V92D), confirming that FtsA(I143L) is a more potent suppressor of FtsQ-related defects (Table 4 and Fig. 7).

DISCUSSION

New alleles of FtsQ define functional domains. In this work, we identified several new lesions that define functional domains of FtsQ involved in divisome assembly (Fig. 1A). The previously identified *ftsQ2* truncation mutant showed that the C-terminal domain, which roughly corresponds to the γ domain, is important for recruitment of downstream proteins. Our analysis refined this picture, identifying the minimal functional length of FtsQ. Our results indicate that a short region of the γ domain near amino acids 250 to 256 is critical for recruitment of FtsL and FtsB. These amino acids (GAAVGW) comprise a cluster of nonpolar residues in a region that is predominantly polar and charged. The importance of this region was reinforced by the isolation of a mutant with a point mutation at amino acid 252 that eliminated the ability of FtsQ to recruit these two proteins. Together with the finding that the γ domain of DivIB from *B. subtilis* is very sensitive to proteolytic degradation (32), these results suggest a model in which the γ domain of FtsQ is unstructured until FtsQ interacts with FtsL and FtsB. In vitro analysis of FtsQ purified in the presence or absence of FtsL/FtsB may be informative in testing this model.

Two of our nonlethal lesions, L55P and R196W, also appeared to disrupt interactions with FtsL and FtsB to some degree. Both mutant proteins localized with wild-type efficiency and showed some level of FtsI recruitment upon initial inspection. However, quantitation of recruitment of FtsI by FtsQ(L55P) and FtsQ(R196W) when single copies were expressed revealed significant recruitment defects compared to FtsQ(WT). The finding that L55P and L60P have similar primary structures but have divergent phenotypes is surprising, yet it is consistent with the fact that L60P, but not L55P, is predicted to be part of the α domain. Based on sequence alignments with DivIB, the R196W mutation is in a relatively nonconserved loop linking strands β4 and β5 (Fig. 1B) (32). Our results suggest that this loop contributes to interactions with downstream proteins.

We also identified two mutants, L60P and V92D, which exhibit defects in localization. Since these mutants localize poorly to midcell, it is not surprising that they do not recruit downstream proteins efficiently. The finding that they recruit downstream proteins at all, given their localization defects, suggests that recruitment activity is not compromised. This apparent paradox is particularly true for L60P; it almost completely fails to localize, yet it still recruits FtsI to some extent. We noted, however, that an N-terminal GFP fusion enhanced the defects associated with the V92D mutation and the FFQ swap constructs, indicating that GFP may interfere with the amino-terminal targeting signal of FtsQ. A similar phenomenon has been reported previously, in which an N-terminal GFP fusion to FtsQ disrupted the ability of FtsQ when it was overexpressed to suppress an FtsK depletion strain (16). Thus, our use of GFP to score localization probably overstates the degree of the localization defect.

Both L60 and R196 are in the predicted POTRA repeat-

containing α domain of FtsQ (33), and thus our results provide the first indication that this domain has a functional role in division. Although the exact function of POTRA repeat domains is unclear, several of these domains have been shown to bind translocation substrates (17), leading us to imagine that such a peptide binding activity in the FtsQ α domain could mediate midcell targeting.

Finally, we uncovered a role for the amino-terminal region of FtsQ in targeting FtsQ to midcell and showed that this targeting requires at least some portion of the cytoplasmic domain. Although essential for neither the function nor the localization of the wild-type FtsQ protein, this targeting role became apparent when we compromised the dominant targeting motif in the α domain. Thus, multiple regions within FtsQ appear to act cooperatively to localize this protein to midcell. A recent report showed that this region of FtsQ is also necessary and sufficient for multicopy suppression of a Δ*ftsK* deletion allele (16). Taken together, these results clearly demonstrate that this region is involved in divisome assembly.

Similar observations of cooperativity among targeting domains have been made for several of the bitopic membrane proteins. For example, FLL is a nonfunctional swap construct in which the cytoplasmic sequence of FtsL is replaced by the 5′ cytoplasmic region of MalF. This construct does not localize. However, we found that introduction of a mutation in the periplasmic region of FtsL distal to the membrane restores the function (N. Buddelmeijer and J. Beckwith, unpublished results). Thus, in these similar but diverse phenomena we found that the proteins do not associate simply via single points of attachment. Rather, association is governed by multiple interactions using multiple domains, perhaps with multiple proteins.

Mutation in interaction domain 1C of FtsA. In a screen for suppressors of the recruitment-defective allele *ftsQ*(*V92D*), we isolated a novel allele of *ftsA*, *ftsA*(*I143L*). We found that rather than specifically compensating for the V92D lesion in FtsQ, *ftsA*(*I143L*) is capable of rescuing a broad array of division defects, including various lesions in *ftsQ* and in *ftsK* and *zipA* deletion mutants. These characteristics are similar to those of a recently isolated suppressor of a Δ*zipA* mutation, *ftsA*(*R286W*) (also known as *ftsA**). However, although the two FtsA mutant alleles are able to rescue similar sets of division defects, as we show here in a direct comparison, the efficiencies with which they do so differ.

We considered two possible models to explain suppression. The mutants could directly enhance interactions between FtsA and downstream proteins, or the mutants could stabilize and/or alter the structure of the Z-ring such that it becomes a more potent scaffold for assembly. Unfortunately, experiments described here and elsewhere are not sufficient to reveal the mechanism by which the FtsA alleles suppress the defects.

The positions of the two mutations in FtsA, which are at opposite ends of the FtsA protein, raise the possibility that they may utilize distinct mechanisms. Isoleucine 143 is in domain 1C, a domain which is conserved among FtsA proteins and which differentiates FtsA from other actin superfamily members (Fig. 8A and B). This domain has been directly implicated in recruitment of downstream division proteins (11, 31) and contains an SHS2 fold, which is thought to mediate protein interactions among a variety of proteins, including components of eukaryotic RNA polymerase (1, 7). Based on the structure of FtsA from *Thermotoga* (36), I143, along with two other amino acids, is part of a triad of aliphatic residues that appear to stabilize a connecting loop in the SHS2 fold (Fig. 8B and C). In contrast, R286W is in strands S12 and S13 of domain 2A. Deletion of these strands results in aberrant Z-ring formation, yet cells are able to divide and recruitment of downstream proteins is normal (31).

On the other hand, FtsA is an actin homologue, and FtsA from at least one species polymerizes in vitro in a head-to-tail fashion in a manner similar to that exhibited by actin (26). In such an arrangement, both mutations are at the proposed dimer interface and thus should be in a position to alter FtsA polymerization, which could have dramatic effects on Z-ring formation, interactions with late proteins, or both.

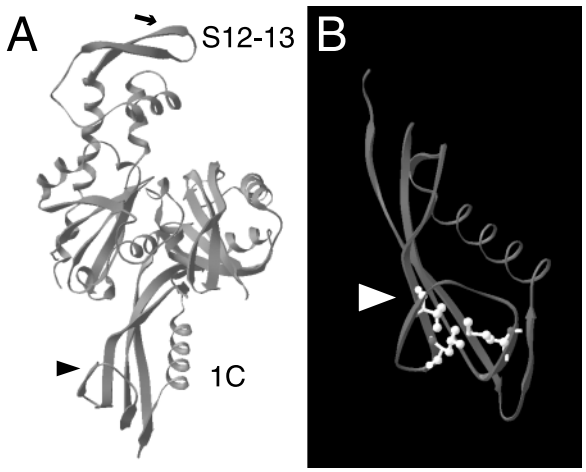

C

T.maritima	PLHIFSKRYLLDDERI**V**FNPLDMKASK
E.coli	VLHVIPQEYAIDYQEG**I**KNPVGLSGVR
S.typhimurium	VLHVIPQEYAIDYQEG**I**KNPVGLSGVR
Y.pestis	ILHVIPQEYAIDYQEG**I**KNPVGLSGVR
V.cholerae	ILHVIPQEFTIDYQEG**I**KNPLGLSGVR
H.influenzae	LLHVIPQEYAVDRQMN**I**KNPLGLQGVR
P.aeruginosa	VLHTLAQDYVIDNQEG**V**REPLGMSGVR
L.pneumophila	ILHILPQEFIIDHQGS**I**REPIGMAGVR
B.mallei	VLHILTQEFIIDGQED**V**REPIGMSGIR
B.pertussis	VLHVLTQEFIVDGQED**I**REPIGMSGLR
G.sulfurreducens	VIHILPQEFIIDDQDG**I**REPLGMSGVR
N.meningitidis	ILDAVVQDYIIDTQLG**V**REPIGMSGVR
B.subtilis	IVDVIPKQFIVDGRDE**I**TDPKKMLGVR
L.monocytogenes	IINTIPDQFVVDGLTG**I**TDPRGMIGVR
E.faecalis	IVAILPQDFTVDGFEG**I**KDPRGMLGVR
S.aureus	VINVFPIRFIVDKENE**V**SDPKELIARH
S.pyogenes	VISLVPEEFIVDGFQG**I**RDPRGMMGIR
B.bacteriovorus	VLHVLPREFKVDGQDG**I**TDPIGMSGIR
D.radiodurans	ILHTIPQEYVVDGQEG**I**KNPVGMHGVR
A.tumefaciens	ILHSLPTGYSLDGERG**I**RDPLSMYGDL
R.sphaeroides	VLHAQPVNFALDHRTG**L**GDPRGQIGNR
C.jejuni	IIHVLPYNFKVNDLEH**V**DDPLGMSGNR

FIG. 8. FtsA structure and sequence alignment. (A) Structure of FtsA from *Thermotoga aquaticus* (36). The positions of domain 1C and strands S12 and S13 are indicated. The positions corresponding to I143 and T286 of *E. coli* are indicated by an arrowhead and an arrow, respectively. (B) Triad of aliphatic amino acids (white) in a close-up of domain 1C. The amino acid corresponding to I143 (in this case Val) is indicated by an arrowhead. (C) Alignment for the loop region from domain 1C. The aliphatic triad is indicated by arrowheads. I143 is in the second position and is indicated by a black arrowhead, while the first and third positions are indicated by gray arrowheads.

Regardless of the precise mechanisms utilized by the two FtsA mutants, we propose that the result is likely the same. Given the complex set of observed connections between cell division proteins, particularly between Z-ring-associated proteins and late proteins (14, 25), and the hierarchy of localization exhibited by the proteins, it is likely that recruitment of late proteins to the Z-ring is mediated by a network of interactions, any one of which is not sufficient on its own to promote recruitment. If this model is correct, either increasing Z-ring density at midcell (and therefore increasing the number of putative binding sites for late proteins) or strengthening interactions between a Z-ring component such as FtsA and late proteins would be predicted to increase the net affinity between the Z-ring and late proteins. Such a model would also explain the abilities of both FtsA suppressor mutants to suppress defects in Z-ring formation (Δ*zipA*) and in assembly of late division proteins (*ftsQ**). Further study of disruptions of the interface between the Z-ring and late proteins and the mechanisms underlying suppression of these defects should provide insight into this critical joint in the assembly of the division machinery.

ACKNOWLEDGMENTS

We thank members of the Beckwith laboratory for critical comments and general assistance. We are especially grateful to Nienke Buddelmeijer, Mark Gonzalez, and Laura Burrack for helping to spearhead initial forays into wrinkled colonies. B. Geissler and B. Margolin graciously provided the *ftsA*(*R286W*) mutant strain.

N.W.G. was supported by a Howard Hughes Predoctoral Fellowship. This work was supported by grant GM38922 from the National Institute of General Medical Sciences. J.B. is an American Cancer Society Professor.

REFERENCES

1. **Anantharaman, V., and L. Aravind.** 2004. The SHS2 module is a common structural theme in functionally diverse protein groups, like Rpb7p, FtsA, GyrI, and MTH1598/TM1083 superfamilies. Proteins **56:**795–807.
2. **Bi, E. F., and J. Lutkenhaus.** 1991. FtsZ ring structure associated with division in *Escherichia coli*. Nature **354:**161–164.
3. **Boyd, D., D. S. Weiss, J. C. Chen, and J. Beckwith.** 2000. Towards single-copy gene expression systems making gene cloning physiologically relevant: lambda InCh, a simple *Escherichia coli* plasmid-chromosome shuttle system. J. Bacteriol. **182:**842–847.
4. **Buddelmeijer, N., M. E. Aarsman, A. H. Kolk, M. Vicente, and N. Nanninga.** 1998. Localization of cell division protein FtsQ by immunofluorescence microscopy in dividing and nondividing cells of *Escherichia coli*. J. Bacteriol. **180:**6107–6116.
5. **Buddelmeijer, N., and J. Beckwith.** 2002. Assembly of cell division proteins at the *E. coli* cell center. Curr. Opin. Microbiol. **5:**553–557.
6. **Buddelmeijer, N., and J. Beckwith.** 2004. A complex of the *Escherichia coli* cell division proteins FtsL, FtsB and FtsQ forms independently of its localization to the septal region. Mol. Microbiol. **52:**1315–1327.
7. **Bushnell, D. A., and R. D. Kornberg.** 2003. Complete, 12-subunit RNA polymerase II at 4.1-A resolution: implications for the initiation of transcription. Proc. Natl. Acad. Sci. USA **100:**6969–6973.
8. **Chen, J. C., D. S. Weiss, J. M. Ghigo, and J. Beckwith.** 1999. Septal localization of FtsQ, an essential cell division protein in *Escherichia coli*. J. Bacteriol. **181:**521–530.
9. **Chen, J. C., and J. Beckwith.** 2001. FtsQ, FtsL and FtsI require FtsK, but not FtsN, for co-localization with FtsZ during *Escherichia coli* cell division. Mol. Microbiol. **42:**395–413.
10. **Chen, J. C., M. Minev, and J. Beckwith.** 2002. Analysis of *ftsQ* mutant alleles in *Escherichia coli*: complementation, septal localization, and recruitment of downstream cell division proteins. J. Bacteriol. **184:**695–705.
11. **Corbin, B. D., B. Geissler, M. Sadasivam, and W. Margolin.** 2004. Z-ring-independent interaction between a subdomain of FtsA and late septation proteins as revealed by a polar recruitment assay. J. Bacteriol. **186:**7736–7744.
12. **Dai, K., Xu, Y., and J. Lutkenhaus.** 1996. Topological characterization of the essential *Escherichia coli* cell division protein FtsN. J. Bacteriol. **178:**1328–1334.
13. **Datsenko, K. A., and B. L. Wanner.** 2000. One-step inactivation of chromosomal genes in *Escherichia coli* K-12 using PCR products. Proc. Natl. Acad. Sci. USA **97:**6640–6645.
14. **Di Lallo, G., M. Fagioli, D. Barionovi, P. Ghelardini, and L. Paolozzi.** 2003. Use of a two-hybrid assay to study the assembly of a complex multicomponent protein machinery: bacterial septosome differentiation. Microbiology **149:**3353–3359.
15. **Geissler, B., D. Elraheb, and W. Margolin.** 2003. A gain-of-function mutation in *ftsA* bypasses the requirement for the essential cell division gene *zipA* in *Escherichia coli*. Proc. Natl. Acad. Sci. USA **100:**4197–4202.
16. **Geissler, B., and W. Margolin.** 2005. Evidence for functional overlap among multiple bacterial cell division proteins: compensating for the loss of FtsK. Mol. Microbiol. **58:**596–612.
17. **Gentle, I. E., L. Burri, and T. Lithgow.** 2005. Molecular architecture and function of the Omp85 family of proteins. Mol. Microbiol. **58:**1216–1225.
18. **Ghigo, J. M., D. S. Weiss, J. C. Chen, J. C. Yarrow, and J. Beckwith.** 1999. Localization of FtsL to the *Escherichia coli* septal ring. Mol. Microbiol. **31:**725–737.
19. **Goehring, N., M. D. Gonzalez, and J. Beckwith.** 2006. Premature targeting of cell division proteins to midcell reveals hierarchies of protein interactions involved in divisome assembly. Mol. Microbiol. **61:**33–45.
20. **Goehring, N. W., and J. Beckwith.** 2005. Diverse paths to midcell: assembly of the bacterial cell division machinery. Curr. Biol. **15:**R514–R526.
21. **Goehring, N. W., F. Gueiros-Filho, and J. Beckwith.** 2005. Premature targeting of a cell division protein to midcell allows dissection of divisome assembly in *Escherichia coli*. Genes Dev. **19:**127–137.
22. **Guzman, L. M., J. J. Barondess, and J. Beckwith.** 1992. FtsL, an essential cytoplasmic membrane protein involved in cell division in *Escherichia coli*. J. Bacteriol. **174:**7716–7728.
23. **Guzman, L. M., D. Belin, M. J. Carson, and J. Beckwith.** 1995. Tight regulation, modulation, and high-level expression by vectors containing the arabinose PBAD promoter. J. Bacteriol. **177:**4121–4130.
24. **Guzman, L. M., D. S. Weiss, and J. Beckwith.** 1997. Domain-swapping analysis of FtsI, FtsL, and FtsQ, bitopic membrane proteins essential for cell division in *Escherichia coli*. J. Bacteriol. **179:**5094–5103.
25. **Karimova, G., N. Dautin, and D. Ladant.** 2005. Interaction network among *Escherichia coli* membrane proteins involved in cell division as revealed by bacterial two-hybrid analysis. J. Bacteriol. **187:**2233–2243.
26. **Lara, B., A. I. Rico, S. Petruzzelli, A. Santona, J. Dumas, J. Biton, M. Vicente, J. Mingorance, and O. Massidda.** 2005. Cell division in cocci: localization and properties of the *Streptococcus pneumoniae* FtsA protein. Mol. Microbiol. **55:**699–711.
27. **Mazouni, K., F. Domain, C. Cassier-Chauvat, and F. Chauvat.** 2004. Molecular analysis of the key cytokinetic components of cyanobacteria: FtsZ, ZipN and MinCDE. Mol. Microbiol. **52:**1145–1158.
28. **Miller, J. H.** 1992. A short course in bacterial genetics: a laboratory manual and handbook for *Escherichia coli* and related bacteria. Cold Spring Harbor Laboratory Press, Cold Spring Harbor, N.Y.
29. **Pichoff, S., and J. Lutkenhaus.** 2002. Unique and overlapping roles for ZipA and FtsA in septal ring assembly in *Escherichia coli*. EMBO J. **21:**685–693.
30. **Pichoff, S., and J. Lutkenhaus.** 2005. Tethering the Z ring to the membrane through a conserved membrane targeting sequence in FtsA. Mol. Microbiol. **55:**1722–1734.
31. **Rico, A. I., M. Garcia-Ovalle, J. Mingorance, and M. Vicente.** 2004. Role of two essential domains of *Escherichia coli* FtsA in localization and progression of the division ring. Mol. Microbiol. **53:**1359–1371.
32. **Robson, S. A., and G. F. King** 2006. Domain architecture and structure of the bacterial cell division protein DivIB. Proc. Natl. Acad. Sci. USA **103:**6700–6705.
33. **Sánchez-Pulido, L., D. Devos, S. Genevrois, M. Vicente, and A. Valencia.** 2003. POTRA: a conserved domain in the FtsQ family and a class of beta-barrel outer membrane proteins. Trends Biochem. Sci. **28:**523–526.
34. **Singer, M., T. A. Baker, G. Schnitzler, S. M. Deischel, M. Goel, W. Dove, K. J. Jaacks, A. D. Grossman, J. W. Erickson, and C. A. Gross.** 1989. A collection of strains containing genetically linked alternating antibiotic resistance elements for genetic mapping of *Escherichia coli*. Microbiol. Rev. **53:**1–24.
35. **Thanedar, S., and W. Margolin.** 2004. FtsZ exhibits rapid movement and oscillation waves in helix-like patterns in *Escherichia coli*. Curr. Biol. **14:**1167–1173.
36. **van den Ent, F., and J. Lowe.** 2000. Crystal structure of the cell division protein FtsA from *Thermotoga maritima*. EMBO J. **19:**5300–5307.
37. **van Helvoort, J. M., and C. L. Woldringh.** 1994. Nucleoid partitioning in *Escherichia coli* during steady-state growth and upon recovery from chloramphenicol treatment. Mol. Microbiol. **13:**577–583.
38. **Weiss, D. S., J. C. Chen, J. M. Ghigo, D. Boyd, and J. Beckwith.** 1999. Localization of FtsI (PBP3) to the septal ring requires its membrane anchor, the Z ring, FtsA, FtsQ, and FtsL. J. Bacteriol. **181:**508–520.
39. **Weiss, D. S.** 2004. Bacterial cell division and the septal ring. Mol. Microbiol. **54:**588–597.